Quasi-two-dimensional magnetism in Ru and Rh metal layers sandwiched between graphene sheets

Masatsugu Suzuki* and Itsuko S. Suzuki
Department of Physics, State University of New York at Binghamton, Binghamton, New York 13902-6016

Jürgen Walter†
Department of Materials Science and Processing, Graduate School of Engineering, Osaka University, 2-1, Yamada-oka, Suita, 565-0871, Japan

(Received 19 September 2002; revised manuscript received 6 December 2002; published 10 March 2003)

$4d$ transition-metal- [(TM)= Ru and Rh] metal-graphite (MG) has a unique layered structure, where the TM monolayer is sandwiched between adjacent graphene sheets. The magnetic properties of TM-MG based on natural graphite are investigated using dc and ac magnetic susceptibility. (i) Ru-MG magnetically behaves like a quasi-two-dimensional ferromagnet. This compound undergoes successive magnetic phase transitions at T_{cu} ($=16.3\pm0.2$ K) and T_{cl} ($=12.8\pm0.3$ K). The origin of two phase transitions in Ru-MG is similar to that in stage-2 $CoCl_2$ graphite intercalation compound ($T_{cu}=8.9$ K and $T_{cl}=6.9$–7.1 K), where the ferromagnetic layers are antiferromagnetically stacked along the c axis. The low-temperature phase below T_{cl} may be a reentrant spin-glass-like phase where the antiferromagnetic phase and spin-glass phase coexist. (ii) Rh-MG exhibits a superparamagnetic behavior. A ferromagnetic blocked state is formed below 9.7 K. The zero-field-cooled susceptibility shows a broad peak around 9.7 K. The irreversible effect of magnetization is observed below 13.5 K. The relaxation time obeys the Arrhenius law for thermal activation.

DOI: 10.1103/PhysRevB.67.094406 PACS number(s): 75.70.Ak, 75.75.+a, 75.20.−g, 75.30.Cr

I. INTRODUCTION

The $4d$ transition metals (TM's) Ru and Rh have large paramagnetic susceptibility with an enhanced Stoner factor $s=1/[1-J_0N(E_F)]$, where J_0 is an exchange parameter and $N(E_F)$ is an electron density of states (DOS) at the Fermi energy E_F. However, these metals are still paramagnetic because the Stoner criterion for the occurrence of ferromagnetism $[J_0N(E_F)>1]$ is not satisfied. For Rh, for example, E_F is located immediately below a sharp leading peak.[1] However, these TM's might have ferromagnetic order, if properly synthesized at the nanometer scale, i.e., (i) small clusters with nanoscale size and (ii) monolayers of these elements epitaxially formed on an adequate nonmagnetic substrate. The possible ferromagnetic (FM) order in such systems is due to the reduced dimensionality, the reduced coordination number, and the enhanced lattice constant. For small clusters, Cox *et al.*,[2] for example, have observed that Rh clusters (Rh_N) with $N=12$–32 show superparamagnetic behavior at 93 K. Inside clusters, Rh magnetic moments are ferromagnetically aligned. Two-dimensional (2D) ferromagnetism in the TM monolayer deposited on Ag(001) or Au(001) surfaces has been theoretically predicted.[3–7] The magnetic moment per atom varies between $0.6\mu_B$ and $1\mu_B$ for Rh and $1.7\mu_B$ for Ru. Experimentally, however, FM long-range order has never been observed in these systems, to our best knowledge.[8,9] This is due to the possible diffusion of TM atoms into the noble-metal substrate. Graphite has been suggested as an alternative substrate, because the TM atoms diffuse much less into it. The graphite C(0001) surface is known to be very flat and it has only a small band overlap with the transition metal d bands. Pfandzelter *et al.*[10] have reported 2D FM order in a Ru monolayer on a graphite C(0001) surface of highly oriented pyrolytic graphite (HOPG). Using Auger electron spectroscopy, they have found that a nonzero in-plane spin polarization appears below 250 K. Motivated by this experiment, Chen *et al.*[11] and Krüger *et al.*[12] have discussed the possible $4d$ magnetism of the TM monolayer on the graphite C(0001) surface. They have shown that the magnetic properties of the system TM/C(0001) are dependent on (i) the in-plane structure of TM atoms and (ii) the TM-C interlayer distance d_c. Krüger *et al.*[12] have assumed a superstructure of the TM atoms which is partly commensurate with that of the graphite substrate. Small magnetic moments can survive for Ru and Rh,[11,12] while the magnetism of Pd is completely diminished.[11] That only Ru and Rh are ferromagnetic could be due to the DOS at E_F which is much larger than that of the other $4d$ metals. So they have the tendency for ferromagnetism according to the Stoner criterion.

The TM metal-graphite (MG) has a unique layered structure, where a TM monolayer is sandwiched between adjacent graphene layers. Ideally these sandwiched structures are stacked along the c axis, forming a staging structure which is similar to that observed in graphite intercalation compounds (GIC's). It is expected that TM-MG's magnetically behave like a quasi-2D magnet. The adjacent TM layers are coupled through very weak interplanar interactions. The magnetism of the TM layers in TM-MG's may be partly similar to that of the TM monolayer/C(0001). In this paper we study the magnetic properties of TM-MG's based on natural graphites using superconducting quantum interference device (SQUID) dc and ac magnetic susceptibility. We show that Ru-MG undergoes magnetic phase transitions at T_{cu} ($=16.3\pm0.2$ K) and T_{cl} ($=12.8\pm0.3$ K). The origin of these phase transitions in Ru-MG is similar to those in stage-2 $CoCl_2$ GIC's ($T_{cu}=8.9$ K and $T_{cl}=6.9$–7.1 K).[13–16] The magnetic phase transitions of stage-two $CoCl_2$ GIC will be briefly described in Sec. II A. The 2D FM layers are antiferromagnetically stacked along the c axis. The interme-

diate phase between T_{cu} and T_{cl} is a 2D FM phase. The low-temperature phase below T_{cl} may be a reentrant spin-glass (RSG) phase, which is the mixed phase of a spin-glass (SG) phase and a three-dimensional (3D) antiferromagnetic (AF) phase established through a very weak AF interplanar interaction.

In contrast, the magnetism of Rh-MG is much weaker than that of Ru-MG. We show that Rh-MG exhibits a superparamagnetic behavior. A FM blocked state is formed below 9.7 K. The observed relaxation behavior and the irreversible effect of magnetization, which are characteristics of superparamagnets, are discussed in terms of the Néel blocking model[17,18] (see Sec. II B).

II. BACKGROUND

A. RSG phase in stage-2 $CoCl_2$ GIC (Refs. 15 and 16)

In order to facilitate the comparison of our results on Ru-MG with those of stage-2 $CoCl_2$ GIC, we present a brief review of the magnetic phase transitions of stage-2 $CoCl_2$ GIC.[15,16] Stage-2 $CoCl_2$ GIC magnetically behaves like a quasi-2D XY-like ferromagnet with a very weak AF interplanar exchange interaction. It undergoes magnetic phase transitions at T_{cu} (=8.9 K) and T_{cl} (=6.8–7.2 K). (i) The absorption χ'' consists of three peaks at T_{cl}, T_p (=8.4 K), and T_{cu} ($T_{cl}<T_p<T_{cu}$). The peak temperature T_{cl} increases with increasing f from 6.8 K at 0.01 Hz to 7.2 K at 1 kHz, while T_p and T_{cu} remain unchanged. (ii) The dispersion χ' shows a single peak at T_p which is independent of f for $0.01 \leqslant f \leqslant 1000$ Hz. (iii) The deviation of the zero-field-cooled (ZFC) susceptibility χ_{ZFC} at an external magnetic field ($H=1$ Oe) along the c plane (perpendicular to the c axis) from the field-cooled (FC) susceptibility χ_{FC} occurs below 18.8 K well above T_{cu}. (iv) The nonlinear ac magnetic susceptibility χ_3' exhibits a small positive peak around T_{cl}. (v) The relaxation time τ is described by a power-law form

$$\tau = \tau_0^*(T/T^* - 1)^{-x}, \tag{1}$$

where $x=7.55\pm1.87$, T^* ($=6.71\pm0.08$ K) is a finite spin-freezing temperature, and τ_0^* [$=2.06\pm0.05)\times10^{-13}$ sec] is a characteristic time. The value of T^* is very close to T_{cl}. The value of x is in good agreement with the theoretical prediction by Ogielski[19] from Monte Carlo simulation of a 3D ($\pm J$) Ising SG model with short-range interactions: $x=7.9\pm1.0$.

Based on the above experimental results, the magnetic phase transitions of stage-2 $CoCl_2$ GIC can be understood as follows. The $CoCl_2$ intercalate layers are formed of small islands whose diameters are on the order of 450 Å.[13,14] The nearest-neighbor spins inside islands are ferromagnetically coupled with FM intraplanar exchange interactions. On approaching T_{cu} from the high-T side, spins come to order ferromagnetically inside islands. At T_{cu} these FM islands continue to order over the same layer through interisland interactions (mainly ferromagnetic), forming a 2D FM long-range order. Below T_{cl} a 3D-like AF long-range order is established through effective AF interplanar interactions between spins in adjacent intercalate layers. In fact the low-temperature phase below T_{cl} is a RSG phase, where the AF phase coexists with a SG phase. The magnetic response of the RSG phase has been theoretically discussed by Takayama[20] using a molecular field theory. The main predictions are as follows. (i) Both the linear dc susceptibility χ_1 and the nonlinear dc susceptibility χ_3 exhibit positive cusps at T_{RSG}. (ii) Both χ_1 and χ_3 decrease quite significantly with decreasing T below T_{RSG}. (iii) The relaxation time τ diverges at T_{RSG}.

B. Néel blocking model (Refs. 17 and 18)

We consider a system consisting of isolated uniaxial single-domain FM clusters where many spins are included. At temperatures much lower than the intrinsic ordered temperature of the bulk system, the magnetic moments of the spins inside each cluster are aligned along the same direction, forming a FM cluster. The magnetic behavior of this system depends on the relative magnitude of the thermal energy (k_BT) with respect to the height of the energy barrier (ΔE_a) which is given by the product of the uniaxial anisotropy (K_u) and the volume (V) of the cluster. When $k_BT \gg \Delta E_A$, the magnetization vector of a cluster can rotate in response to a change in temperature or magnetic field, so that a thermal equilibrium is established within a very short time. The clusters, which are ferromagnetically ordered, exhibit a superparamagnetic behavior. There is no interaction between clusters. The magnetization of the superparamagnet is considerably larger than that of atomic paramagnetism and shows a tendency to saturate in rather small H. When $k_BT \ll \Delta E_A$, the presence of the anisotropy barrier impedes the rotation of the magnetization vector and the system approaches equilibrium with a relaxation time τ given by

$$\tau = \tau_0 \exp(\Delta E_a / k_B T), \tag{2}$$

[thermal activation (Arrhenius law)],[17,18] where τ_0 is the characteristic relaxation time. For the dc magnetization measurement, a blocking temperature $T_B(\mathrm{dc})$ is defined as $T_B(\mathrm{dc}) = \Delta E_a / [\ln(\tau_m/\tau_0)k_B]$ from the condition ($\tau=\tau_m$), where τ_m is the time taken for the dc measurement and is usually chosen as 10^2 sec. For $T>T_B(\mathrm{dc})$ the single-domain clusters exhibit superparamagnetic behavior. For $T<T_B(\mathrm{dc})$ the magnetic moments of clusters are blocked in the direction of the anisotropy axis, forming a FM blocked state, since they are unable to rotate over the energy barrier in the time scale of the measurement.

III. EXPERIMENT

dc and ac magnetic-susceptibility measurements of Ru- and Rh-MG's were carried out using a SQUID magnetometer (MPMS XL-5, Quantum Design) with an ultralow-field capability. The sample used in the present work consists of many small flakes, where each flake has a well-defined c axis. The system may be regarded as a powder as a whole in the sense that the direction of the c axis cannot be defined.

The sample of Ru-MG was made in two steps: (i) the preparation of the $RuCl_3$ GIC and (ii) the synthesis of

Ru-MG from the $RuCl_3$ GIC. The $RuCl_3$ GIC, as a precursor, was synthesized by heating a mixture of natural graphite (from Graphitwerke Kropfmühl, Germany) and $RuCl_3$ in a chlorine gas atmosphere. The reaction was continued at 400 °C for three days. It was confirmed from $(00L)$ x-ray diffraction that the sample was dominated by a stage-two fraction with the *c*-axis repeat distance 12.60 Å. Note that for the stage-2 $RuCl_3$ GIC there are two graphene layers between adjacent $RuCl_3$ layers. Ru-MG was prepared from the reduction of the $RuCl_3$ GIC under the flow of hydrogen gas at 200 °C. The structure of samples was studied using a Hitachi H-800 transmission-electron microscope with accelerating voltage 200 kV. Selected-area electron-diffraction (SAED) patterns in Ru-MG show polycrystalline diffraction rings, suggesting that Ru layers are formed of Ru clusters. The average in-plane size of Ru clusters was not determined because of the statistical uncertainty.

The sample preparation of Rh-MG was similar to that of Ru-MG. $RhCl_3$ GIC samples were prepared by heating a mixture of pristine $RhCl_3$ and natural graphite at 240 °C in a chlorine gas atmosphere. The reaction was continued for three days. Reduction of the $RhCl_3$ GIC was made at room temperature in Li-diphenylide in tetrahydrofuran (THF) for two days. The SAED pattern in Rh-MG consists of weak Bragg reflections arising from face-centered-cubic (fcc) Rh and strong Bragg reflections arising from 2D aggregates with $(2\times a_G)$ and $(3\times a_G)$ superstructures, where a_G is the in-plane lattice constant of the pristine graphite. The average in-plane size of Rh clusters is (60 ± 45) Å. The details of the structural analysis are given elsewhere.[21]

IV. RESULT

A. Ru-MG

The results from magnetic measurements of Ru-MG are as follows, suggesting that Ru-MG undergoes successive magnetic phase transitions at T_{cu} and T_{cl}. Figure 1 shows the temperature (T) dependence of χ_{ZFC} and χ_{FC} for Ru-MG at various magnetic fields (H). The measurements were carried out as follows. After the sample was cooled from 298 to 1.9 K at $H=0$ (in a strict sense, a very weak remanent field less than 3 mOe), H was applied at $T=1.9$ K. The susceptibility χ_{ZFC} was measured with increasing T from 1.9 to 40 K. After the sample was annealed at 100 K for 20 min in the presence of H, χ_{FC} was measured with decreasing T from 40 to 1.9 K. In Fig. 2 we show the T dependence of the difference $\delta\chi$ defined by $\delta\chi=\chi_{FC}-\chi_{ZFC}$ at various H. We find that χ_{ZFC} starts to deviate from χ_{FC} below a characteristic temperature which decreases with increasing H. Figure 3 shows the T dependence of the derivatives $d\chi_{ZFC}/dT$ and $d\delta\chi/dT$ for Ru-MG at various H. The susceptibility χ_{ZFC} at $H=20$ Oe shows a peak at 15.6 K corresponding to the upper critical temperature $T_{cu}(H)$, while $d\chi_{ZFC}/dT$ shows a plateaulike behavior between 9.6 and 12.4 K. The lower critical temperature $T_{cl}(H)$ is included in this temperature range. The derivative $d\chi_{ZFC}/dT$ at $H=10$ Oe (the data are not shown in Fig. 3) shows a plateaulike behavior between 10.4 and 13.2 K, where $T_{cl}(H)=12.8$ K. It is reasonable to assume that the peak temperature of $d\chi_{ZFC}/dT$ corresponds to $T_{cl}(H)$. For a normal antiferromagnet ($\chi=\chi_{FC}=\chi_{ZFC}$) the Néel temperature T_N for the 3D AF order coincides with a peak temperature of $d\chi/dT$ vs T.

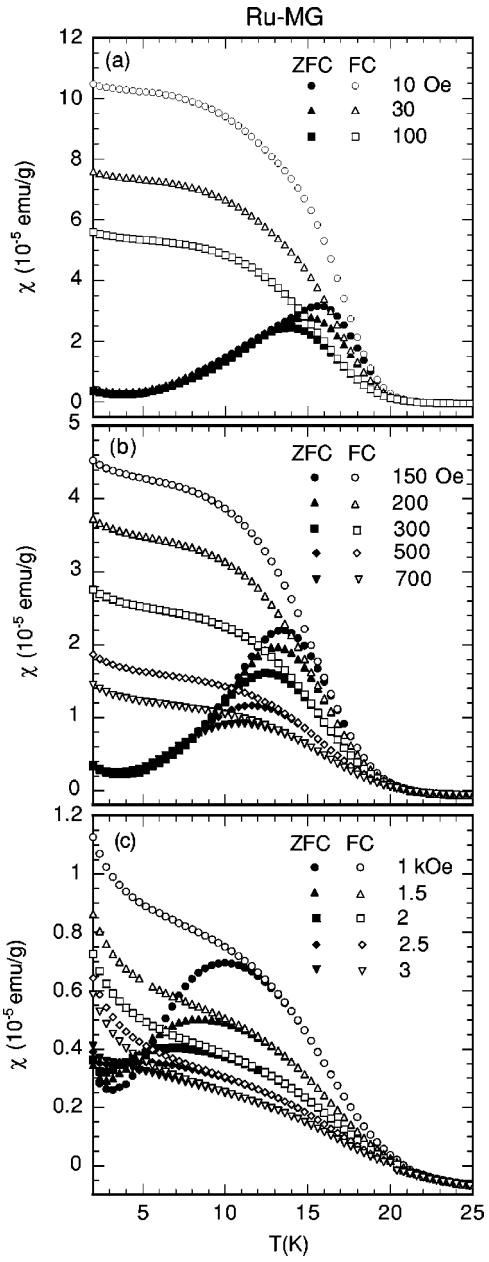

FIG. 1. T dependence of χ_{ZFC} and χ_{FC} for Ru-MG at various H.

The difference of $\delta\chi$ appears below 18.8 K well above $T_{cu}(H)$, indicating that the irreversible effect of magnetization occurs due to possible spin frustration effects. Note that such an irreversibile effect is observed even at $H=3$ kOe. As shown in Fig. 3(a), the local maximum of $d\chi_{ZFC}/dT$ shifts to the low-T side with increasing H, while the local minimum of $d\chi_{ZFC}/dT$ appears around 16 K. As shown in Fig. 3(b), the derivative $d(\delta\chi)/dT$ exhibits a negative local minimum around $T_{cl}(H)$ for $H\geqslant 100$ Oe, which shifts to the low-T side with increasing H.

Figure 4 shows the T dependence of M in ZFC, FC, isothermal remanent, (IR) and thermoremanent (TR) states in

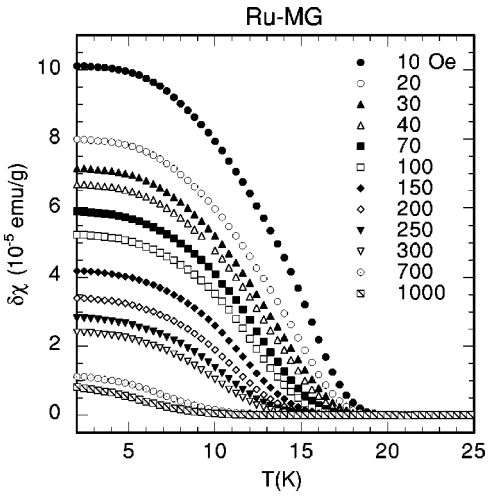

FIG. 2. T dependence of the difference $\delta\chi$ $(=\chi_{FC}-\chi_{ZFC})$ for Ru-MG at various H.

the case of $H=20$ Oe. The measurements were carried out as follows. First, the sample was cooled from 298 to 1.9 K at $H=0$. Then H $(=20$ Oe) was applied. The measurements of M_{ZFC} and M_{IR} were done with increasing T from 1.9 to 35 K. At each T, M_{ZFC} was measured at H and then M_{IR} was measured 100-sec later after the field was changed from H to 0 Oe. Second, the sample was annealed at 100 K for 1200 sec at H. The measurements of M_{FC} and M_{TR} were done with decreasing T from 35 to 1.9 K. At each T, M_{FC} was measured at H and then M_{TR} was measured 100-sec later after the field was changed from H to 0 Oe. The magnetization M_{ZFC} shows a broad peak at 15 K, while M_{IR} exhibits a

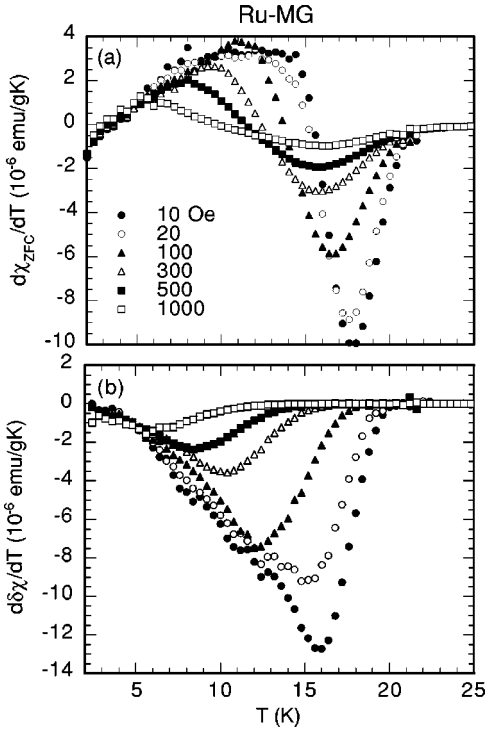

FIG. 3. T dependence of (a) $d\chi_{ZFC}/dT$ and (b) $d\delta\chi/dT$ for Ru-MG at various H, where $\delta\chi=\chi_{FC}-\chi_{ZFC}$.

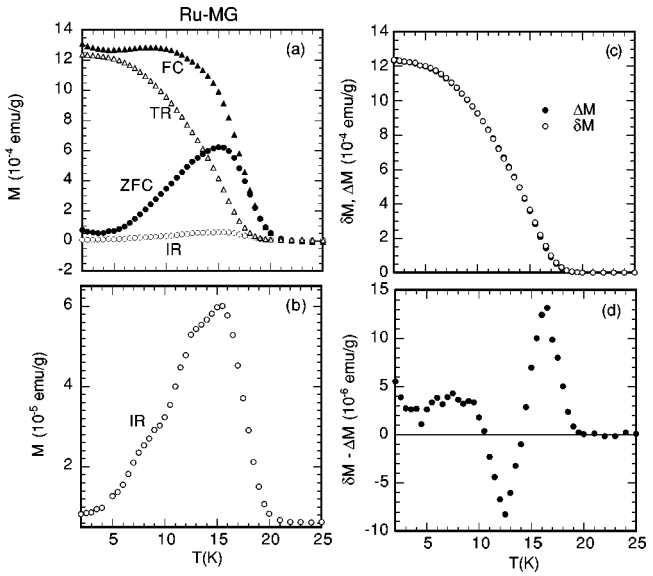

FIG. 4. (a) T dependence of M_{ZFC} and M_{FC} at $H=20$ Oe, and M_{IR} and M_{TR} at $H=0$ for Ru-MG. The definition of M for each state is given in the text. (b) Detail of M_{IR} vs T in (a). (c) δM $(=M_{FC}-M_{ZFC})$ vs T and ΔM $(=M_{TR}-M_{IR})$ vs T. (d) $(\delta M-\Delta M)$ vs T.

peak around 15.5 K and shoulders around 9 and 12 K. The difference δM $(=M_{FC}-M_{ZFC})$ almost coincides with the difference ΔM $(=M_{TR}-M_{IR})$ at any T. Both δM and ΔM appear below 18.5 K. In Fig. 4(d) we make a plot of $(\delta M-\Delta M)$ as a function of T. The difference $(\delta M-\Delta M)$ clearly shows a local maximum at 16.5 K near T_{cu} and a local minimum at 12.5 K near T_{cl}. Similar behaviors are also observed at T_{cu} and T_{cl} in stage-2 $CoCl_2$ GIC.[22] Note that there has been no theoretical explanation for the T dependence of $(\delta M-\Delta M)$ in these systems.

The ac magnetic susceptibility $(=\chi'+i\chi'')$ was measured as a function of frequency (f) at each T in the absence of H, where the amplitude (h) of the ac magnetic field was 3 Oe. After each f scan $(0.1 \leqslant f \leqslant 1000$ Hz), the temperature was increased by $\Delta T=0.5$ K. The same experiment was continued at different T. Figure 5 shows the T dependence of χ' and χ'' at $H=0$ for Ru-MG. The dispersion χ' exhibits a single peak at 16 K, which is independent of f for $0.1 \leqslant f \leqslant 1000$ Hz. In contrast, χ'' at $f=0.1$ Hz exhibits a broad peak at $T_{cu}=16$ K and plateaulike behavior between $T_{pu} \approx 10.5$ K and $T_{pl} \approx 13$ K, where $T_{pl}<T_{cl}<T_{pu}$. The characteristic temperature T_{pl} slightly increases with increasing f from 10.5 K at $f=0.1$ Hz to 12 K at $f=100$ Hz, suggesting the increase of the corresponding relaxation time τ with decreasing T. In the present work, however, no T dependence of τ can be exactly obtained from the data of T_{pl} vs T for the analysis. In contrast to T_{pl}, the temperatures T_{pu} and T_{cu} remain unchanged when f increases. Note that the T dependence of χ'' for $f=100$ Hz is still similar to that for $f=10$ Hz but the magnitude of χ'' at $f=100$ Hz is almost twice larger than that at $f=10$ Hz at the same T near T_{cu} and T_{cl}.

Figure 6 shows the T dependence of χ_{FC} for Ru-MG. It was measured with decreasing T from 298 to 2 K in the

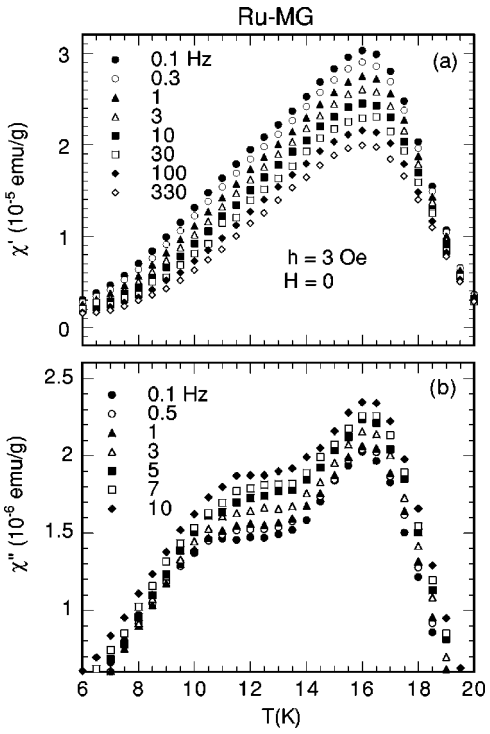

FIG. 5. T dependence of (a) χ' and (b) χ'' for Ru-MG at various f. $h=3$ Oe. $H=0$.

presence of H (=5 and 10 kOe). The susceptibility χ_{FC} is strongly dependent on H for $T\leqslant 20$ K but it is almost independent of H for $T\geqslant 20$ K. The susceptibility χ_{FC} obeys a Curie-Weiss law in the limited temperature range ($20\leqslant T\leqslant 80$ K). The least-squares fit of the data of χ_{FC} vs T to a Curie-Weiss law given by

$$\chi_{FC}=\chi_{FC}^{0}+C_g/(T-\theta) \tag{3}$$

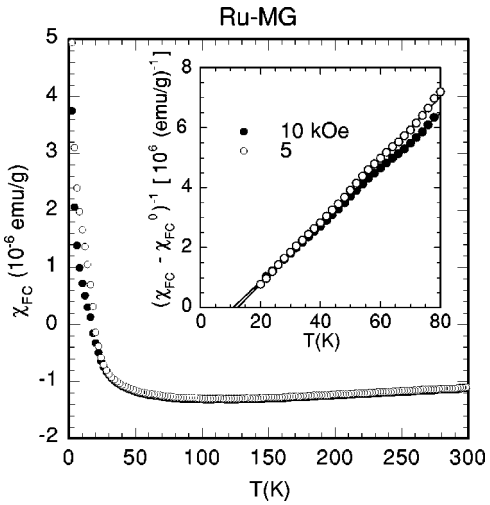

FIG. 6. T dependence of χ_{FC} for Ru-MG at $H=5$ and 10 kOe. The inset shows the T dependence of $(\chi_{FC}-\chi_{FC}^{0})^{-1}$, where χ_{FC}^{0} is the T-independent susceptibility determined from the least-squares fit. The solid lines denote the least-squares fitting curves to Eq. (3).

yields the Curie-Weiss temperature $\theta=12.54\pm 0.10$ K, the Curie-Weiss constant $C_g=(9.57\pm 0.13)\times 10^{-6}$ emu K/g, and the T-independent susceptibility $\chi_{FC}^{0}=(-1.415\pm 0.003)\times 10^{-6}$ emu/g for $H=5$ kOe, and $\theta=10.87\pm 0.09$ K, $C_g=(10.66\pm 0.09)\times 10^{-6}$ emu K/g, and $\chi_{FC}^{0}=(-1.451\pm 0.002)\times 10^{-6}$ emu/g for $H=10$ kOe. The positive sign of θ indicates that the intraplanar interaction between Ru atoms is ferromagnetic. This result is consistent with the theoretical prediction[11,12] that the 2D ferromagnetism exists on the Ru monolayer on the graphite surface C(0001). The susceptibility χ_{FC} exhibits a local minimum ($\approx -1.32\times 10^{-6}$ emu/g) around 100–120 K and slightly increases with further increasing T. The sign of χ_{FC} is still negative at 298 K. The diamagnetic contribution arises from the orbital motions of conduction electrons in the graphite part of Ru-MG, as will be discussed later in Sec. V B. The Curie-Weiss constant C_g is related to the effective magnetic moment P_{eff} by $C_g\approx(P_{eff}^{2}/8)(N_g/N_A)$, where N_A is Avogadro's number and N_g is the number of Ru atoms per gram of the sample. Although N_g is not exactly determined in the present work, the upper limit of P_{eff} can be estimated as follows. The magnetization M_g is given by 3.75×10^{-2} emu/g at $H=10$ kOe and $T=2$ K. This value of M_g is considered to be much smaller than the saturation magnetization given by $M_s=N_g g_J \mu_B J$ (J is the angular momentum quantum number and g_J is the Landé g factor for Ru), leading to $N_g\geqslant 4\times 10^{18}/g_J J$. Then we obtain an inequality for P_{eff}: $P_{eff}\leqslant 3.4(g_J J)^{1/2}$.

B. Rh-MG

The results of magnetic measurements in Rh-MG are as follows, suggesting that Rh-MG shows a superparamagnetic behavior. A FM blocked state is formed below 9.7 K. Figure 7 shows the T dependence of χ_{ZFC} and χ_{FC} at various H for Rh-MG. The measurements were carried out as follows. After the sample was cooled from 298 to 1.9 K at $H=0$, H was applied at $T=1.9$ K. The susceptibility χ_{ZFC} was measured with increasing T from 1.9 to 298 K and sequentially χ_{FC} was measured with decreasing T from 298 to 1.9 K. The susceptibility χ_{ZFC} starts to deviate from χ_{FC} at 298 K, reflecting the frustrated nature of the system. The susceptibility χ_{ZFC} exhibits a local maximum around T_p(ZFC)=9.7 K and a local minimum around 21–22 K at $H=5$ and 10 Oe. This local maximum disappears at H larger than 30 Oe. The susceptibility χ_{FC} does not show any anomaly at T_p(ZFC) and increases with decreasing T. This is in contrast to the T dependence of χ_{FC} observed in a typical SG system, where χ_{FC} is nearly independent of T below the spin freezing temperature T_f. Such a difference between superparamagnetic behavior and SG behavior in χ_{FC} and χ_{ZFC} has been discussed in detail by Bitoh *et al.*[23] It follows that superparamagnetic behavior occurs in Rh-MG. Rh clusters are ferromagnetically ordered. However, there is no interaction between different Rh clusters. Similar superparamagnetic behavior is observed in [tetrakis (dimethylamino) ethylene]-C_{60}.[24] The spins of unpaired electrons localized at the C_{60}^{-} ion are ferromagnetically ordered below T_c (=16 K). A re-

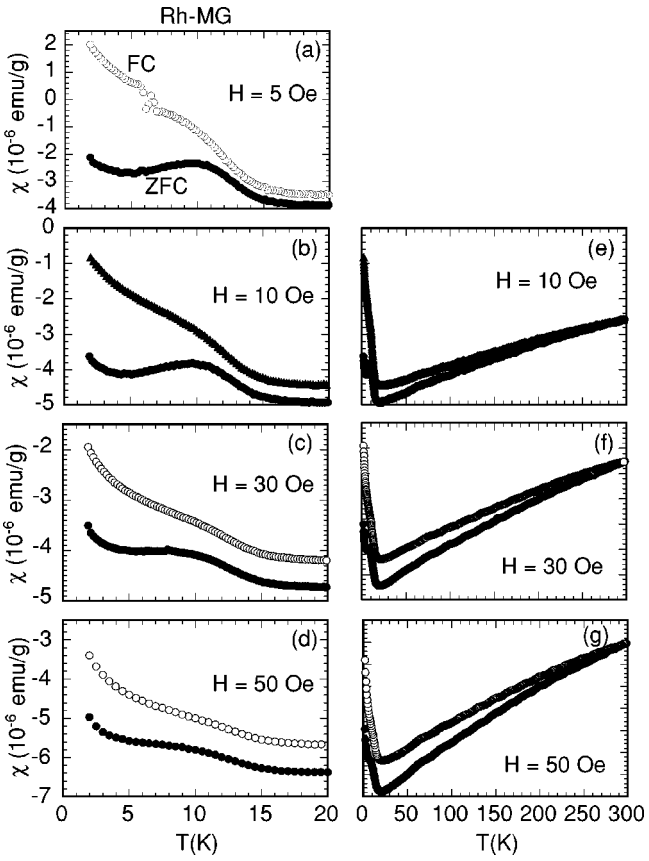

FIG. 7. T dependence of χ_{ZFC} and χ_{FC} at various H for Rh-MG. A part of the data is shown in Ref. 21.

sidual orientation disorder of nearly spherical C_{60} molecules gives rise to characteristics of superparamagnetic behavior.

Figure 8 shows the T dependence of the difference of $\delta\chi$ $(=\chi_{FC}-\chi_{ZFC})$ for Rh-MG. The difference of $\delta\chi$ gradually increases with decreasing T below 298 K. The drastic increase of $\delta\chi$ occurs below a characteristic temperature T_f $=13.5$ K, which is independent of H for $5\leqslant H\leqslant 50$ Oe. The value of T_f is higher than the peak temperature $[T_p(\mathrm{ZFC})]$.

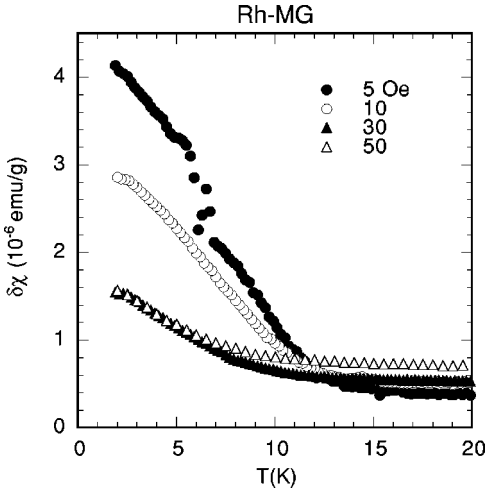

FIG. 8. T dependence of the difference $\delta\chi$ $(=\chi_{FC}-\chi_{ZFC})$ at various H for Rh-MG.

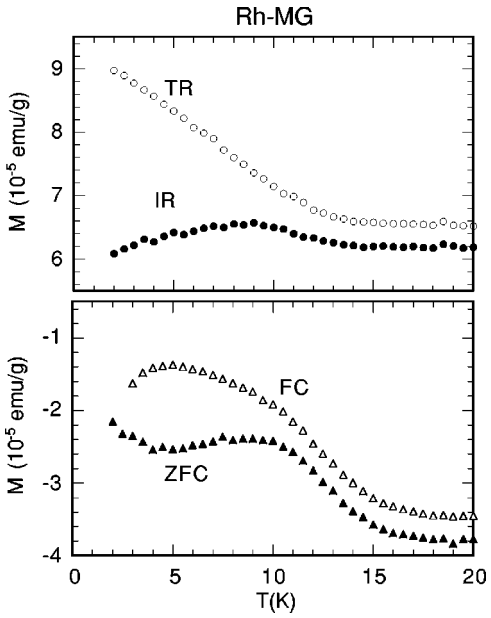

FIG. 9. T dependence of M_{ZFC} and M_{FC} at $H=20$ Oe, and M_{IR} and M_{TR} at $H=0$ for Rh-MG. The detail of the measurement is given in the text.

Figure 9 shows the T dependence of the magnetizations M_{ZFC}, M_{FC}, M_{IR}, and M_{TR}. The ZFC and IR magnetizations were measured as follows. The sample was cooled in $H=0$ from 298 to 1.9 K. At each T in the ZFC process of increasing T $(2\leqslant T\leqslant 50$ K), M_{ZFC} was measured at H $(=20$ Oe) and M_{IR} was measured 10^2-sec later after resetting H to zero. The FC and TR magnetizations were measured as follows. The sample was annealed at 100 K in the presence of H for 20 min. At each T in the FC process of decreasing T $(2\leqslant T\leqslant 50$ K), M_{FC} was measured at H and M_{TR} was measured 10^2-sec later after resetting H to zero. For the superparamagnetic system, it is predicted that the ZFC and FC magnetizations of the system are described by $M_{ZFC}=M_{REV}+M_{IR}$ and $M_{FC}=M_{REV}+M_{TR}$, respectively.[18] Here M_{REV} is the reversible superparamagnetic contribution, while M_{IR} and M_{TR} are the irreversible parts of magnetization. The magnetization M_{IR} is the remanence due to the contribution of the blocked clusters whose moments can rotate over the energy barrier due to the presence of H. The magnetization M_{TR} is the remanence due to the contribution of the clusters that have been blocked in the direction of the cooling H. As shown in Fig. 9, the sign of M_{TR} and M_{IR} is positive, while the sign of M_{ZFC} and M_{FC} is negative. The magnetization M_{TR} drastically decreases with increasing T and is reduced to a constant value at 13.5 K, which is the same as T_f where δ $(=\chi_{FC}-\chi_{ZFC})$ becomes zero. This result gives clear evidence for the occurrence of the FM blocked state of Rh clusters at low T. The magnitude of M_{IR} is much smaller than that of M_{TR}. The magnetization M_{IR} shows a small peak around 9 K and becomes constant above 13.5 K. The magnetization M_{TR} increases with decreasing T until all Rh clusters are blocked. Similar behaviors are observed in fine particles of magnetite (Fe_3O_4).[25]

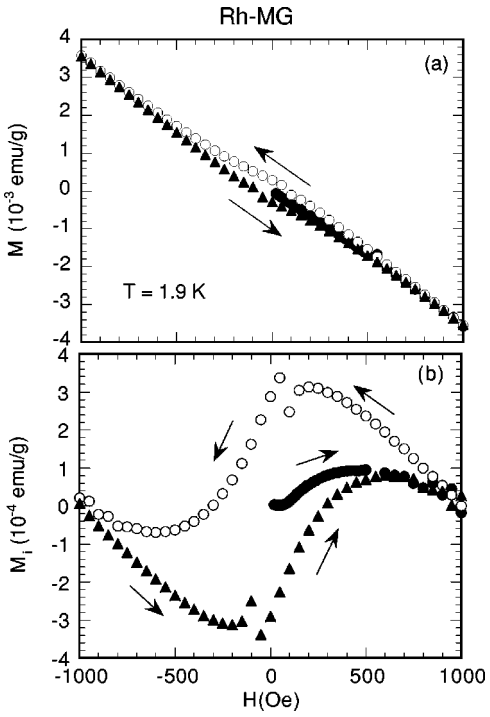

FIG. 10. (a) Hysteresis loop of magnetization M for Rh-MG. $T=1.9$ K. The measurement is made with increasing H from 0 to 1 kOe (closed circles), with decreasing H from 1 kOe to -1 kOe (open circles), and with increasing H from -1 kOe to 1 kOe (closed triangles). (b) Hysteresis loop of M_i $(=M-\chi_d H)$ for Rh-MG. $T=1.9$ K. $\chi_d=-3.58\times10^{-6}$ emu/g. A part of the data is shown in Ref. 21.

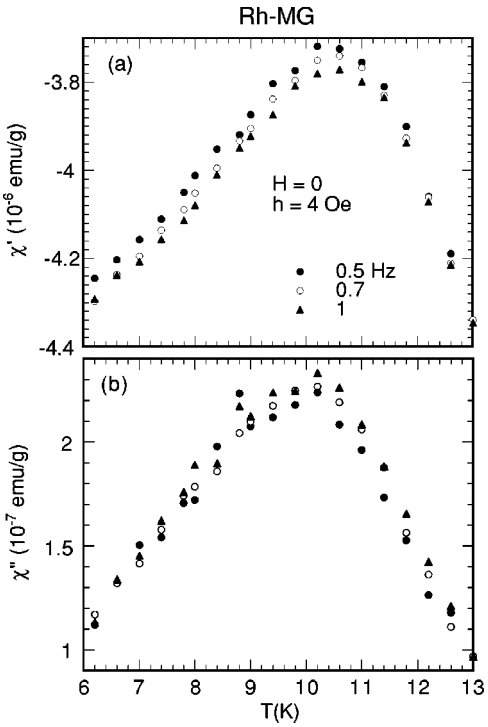

FIG. 11. T dependence of (a) χ' and (b) χ'' at $f=0.5$, 0.7, and 1 Hz for Rh-MG. $H=0$. $h=4$ Oe.

Figure 10 shows the H dependence of the magnetization M at 1.9 K for $-1\leqslant H\leqslant 1$ kOe. The measurement was done after the sample was cooled from 298 to 1.9 K at $H=0$. The curve of M vs H is dominated by a diamagnetic contribution $(=\chi_d H)$. The H dependence of M_i $(=M-\chi_d H)$ is dependent on the choice of χ_d. The shape of M_i vs H with $\chi_d \approx -3.58\times10^{-6}$ emu/g is rather different from that of the usual ferromagnet. A remanent magnetization (M_i at $H=0$) is given by $M_i=2.88\times10^{-4}$ emu/g, suggesting the existence of a FM component in Rh-MG.

Figure 11 shows the T dependence of χ' and χ'' at $f=0.5$, 0.7, and 1 Hz, where $H=0$, $h=4$ Oe. Figure 12 also shows the T dependence of χ' for $0.5\leqslant f\leqslant 7$ Hz. The dispersion χ' exhibits a peak at $T_p(\omega)=10.2$ K at $f=0.5$ Hz, where $\omega=2\pi f$. This peak shifts to the high-T side with increasing f for $0.5\leqslant f\leqslant 7$ Hz. The dispersion χ' still has a peak for $10\leqslant f\leqslant 700$ Hz. However, the peak does not shift with further increasing f and remains unchanged at 11.4 K. Here we assume that these peaks occur when $\omega\tau=1$ for $0.5\leqslant f\leqslant 7$ Hz. The inset of Fig. 12 shows the T dependence of τ, which is obtained from the peak temperature $T_p(\omega)$ of χ' vs T for each f. The relaxation time τ increases with decreasing T. The T dependence of τ will be discussed in Sec. V B.

Figure 13 shows the T dependence of χ'' for $0.5\leqslant f\leqslant 700$ Hz. The absorption χ'' exhibits a very broad peak at $T_p(\omega)=10.2$ K for $0.5\leqslant f\leqslant 10$ Hz. In contrast, it has no peak for $f\geqslant 20$ Hz: it decreases with increasing T. The magnitude of χ'' at 10.2 K linearly increases with increasing f for $0.5\leqslant f\leqslant 1000$ Hz. What happens to χ' and χ'' for $f\geqslant 20$ Hz? For the ac magnetic susceptibility, the corresponding blocking temperature $T_B(\omega)$ is given by $T_B(\omega)/T_B(\mathrm{dc})=\ln(\tau_m/\tau_0)/\ln(1/\omega\tau_0)$. The blocking temperature $T_B(\omega)$ increases with increasing f: $T_B(\omega)\approx 12.6$ K for $f=20$ Hz and $T_B(\omega)=13.5$ K for $f=60$ Hz. The value of $T_B(\omega)$ is comparable to T_f for $f\geqslant 20$ Hz. For $T<T_B(\omega)$ the system is in the FM blocked state.

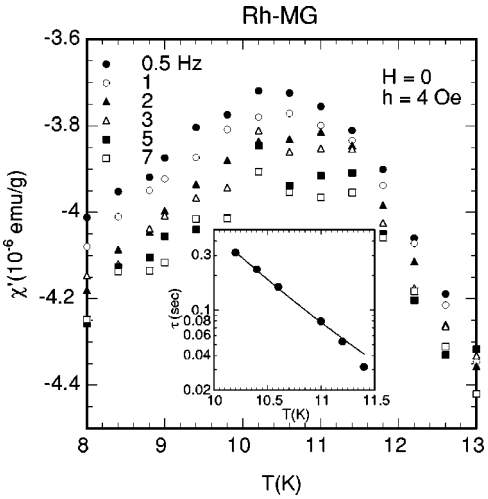

FIG. 12. T dependence of χ' at various f for Rh-MG. $H=0$. $h=4$ Oe. The inset shows the T dependence of τ obtained from the peak temperature of χ' vs T. The solid line is denoted by Eq. (2) with parameters given in the text.

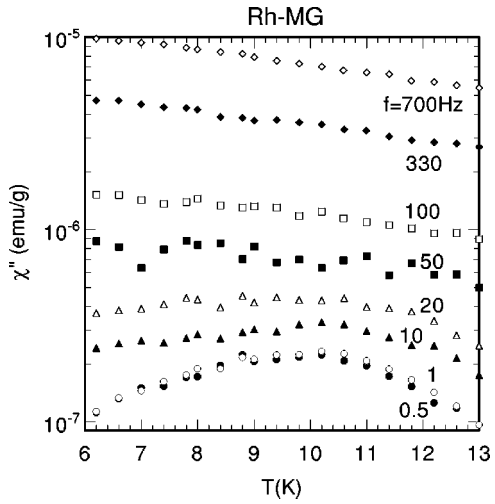

FIG. 13. T dependence of χ'' at various f for Rh-MG. $H=0$. $h=4$ Oe.

Figure 14 shows the T dependence of χ' and χ'' in the presence of various H, where $f=1$ Hz and $h=4$ Oe. At $H=0$ χ' and χ'' show peaks at 10.5 K and 10.0 K, respectively. These peaks completely disappear for $H \geqslant 10$ Oe. The peak of χ'' at $f=1$ Hz shifts to the low-T side with increasing H for $0 \leqslant H \leqslant 5$ Oe: peak temperatures are 9.96 K at $H=0$ and 8.1 K at $H=5$ Oe. Such a shift of the peak temperature is explained by the Néel model,[26] where the blocking temperature $T_B(\omega,H)$ is given by $T_B(\omega,H)/T_B(\omega,H=0)=(1-H/H_K)^2$, where H_K is the mean anisotropy field. The presence of H reduces the height of energy barrier (ΔE_B) over which the moments rotates and consequently

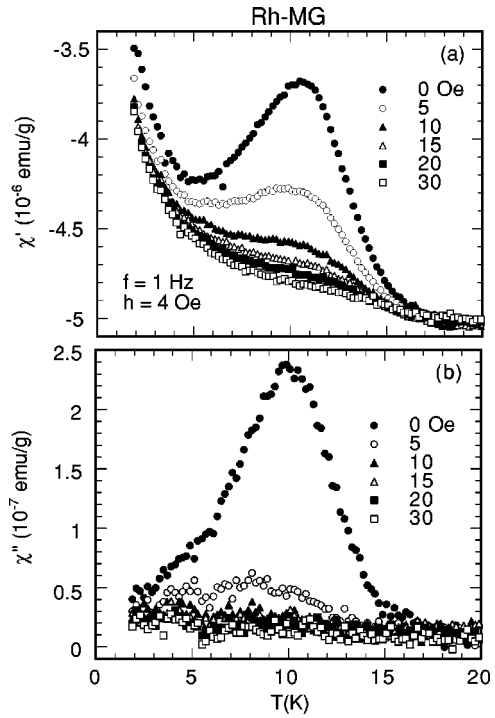

FIG. 14. T dependence of (a) χ' and (b) χ'' at various H for Rh-MG. $f=1$ Hz. $h=4$ Oe.

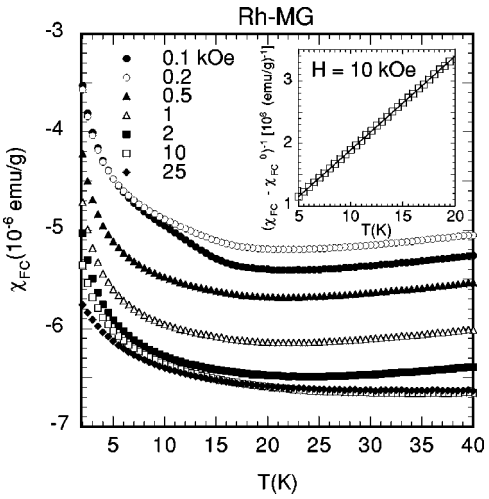

FIG. 15. T dependence of χ_{FC} at various H for Rh-MG. The inset shows the T dependence of $(\chi_{FC}-\chi_{FC}^0)^{-1}$ at $H=10$ kOe, where χ_{FC}^0 is the T-independent susceptibility. The solid line denotes the least-squares fitting curve to Eq. (3).

reduces the blocking temperatures. Using only two data at $H=0$ and 5 Oe, the value of H_K is roughly estimated as $H_K=50$ Oe, where $T_p(\omega,H)$ is assumed to be proportional to $T_B(\omega,H)$.

Figure 15 shows the T dependence of χ_{FC} at high H. The susceptibility χ_{FC} drastically increases with decreasing T at low T, showing a Curie-like behavior in the limited T range ($5 \leqslant T \leqslant 20$ K). The least-squares fit of the data at $H=10$ kOe to Eq. (3) yields the T-independent susceptibility $\chi_{FC}^0=(-6.889\pm0.002)\times10^{-6}$ emu/g, the Curie-Weiss constant $C_g=(6.692\pm0.052)\times10^{-6}$ emu K/g, and the Curie-Weiss temperature $\theta=-2.72\pm0.05$ K. The value of C_g for Rh-MG is smaller than that for Ru-MG. Both χ_{ZFC} and χ_{FC} above 23 K increase with increasing T. They are still negative below 298 K (the data are not shown in Fig. 15), indicating diamagnetic behavior. Here it is interesting to compare our data with that of pristine graphite. The susceptibility of pristine graphite is diamagnetic and anisotropic. Since the magnitude of χ_c along the c axis is much larger than that of χ_a along the c plane for pristine graphite, the orientation average of the susceptibility is given by $(2\chi_a+\chi_c)/3 \approx \chi_c/3$. In the present work, the T dependence of χ_c for the HOPG sample (Union Carbide) was measured at $H=10$ kOe. The susceptibility χ_c increases with increasing T, where $\chi_c=-29.30\times10^{-6}$ emu/g at 30 K and $\chi_c=-18.54\times10^{-6}$ emu/g at $T=298$ K. For comparison, we use the data of χ_{FC} at $H=50$ Oe in Fig. 7(g) for Rh-MG ($\chi_{FC}=-5.64\times10^{-6}$ emu/g at 30 K and -3.02×10^{-6} emu/g at 298 K). We assume that the contribution of graphite to the susceptibility in Rh-MG is described by $\zeta(\chi_c/3)$, where ζ is a parameter. Then the value of ζ (= 0.58) estimated for the data at 298 K is on the same order as that ($\zeta=0.49$) at 30 K. This result suggests that the diamagnetic behavior of χ_{FC} at high-T in Rh-MG is mainly due to the orbital diamagnetism of conduction electrons in graphene layers. This is also the case for Ru-MG (see Fig. 6).

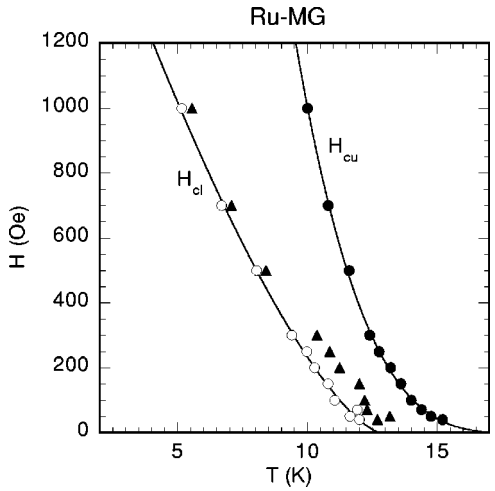

FIG. 16. *H-T* diagram for Ru-MG. The peak temperatures of χ_{ZFC} vs T (closed circles), $d\chi_{ZFC}/dT$ vs T (open circles), and the local-minimum temperature of $d\delta\chi/dT$ vs T (closed triangles) are plotted as a function of H. The solid lines denote the least-squares fitting curves to Eq. (4) with $i=$cu and cl. See the text for details.

V. DISCUSSION

A. Magnetic phase transition in Ru-MG

Figure 16 shows the *H-T* diagram for Ru-MG. The peak temperatures of χ_{ZFC} vs T and $d\chi_{ZFC}/dT$ vs T, and the local-minimum temperature of $d\delta\chi/dT$ vs T are plotted as a function of H. The *H-T* diagram consists of two critical lines H_{cu} and H_{cl}, which correspond to the critical temperatures $T_{cu}(H)$ and $T_{cl}(H)$, respectively. These lines are assumed to be described by a power-law form given by

$$H_i = H_i^*(1 - T/T_i)^{\alpha_i}, \tag{4}$$

where $i=$cu and cl, α_i is an exponent, H_i^* is the characteristic field, and T_i is the critical temperature at $H=0$. The least-squares fit of the data for H_{cu} vs T ($H \leqslant 2$ kOe) obtained from the data of χ_{ZFC} vs T yields $T_{cu}=16.3 \pm 0.2$ K, $\alpha_{cu}=2.06\pm 0.05$, and $H_{cu}^*=6.48\pm 0.05$ kOe. Similarly, the least-squares fit of the data for H_{cl} vs T ($H \leqslant 1$ kOe) obtained from the data of $d\chi_{ZFC}/dT$ vs T yields $T_{cl}=12.8\pm 0.3$ K, $\alpha_{cl}=1.44\pm 0.05$, and $H_{cl}^*=2.08 \pm 0.03$ kOe. The exponent α_{cl} is close to that ($=1.5$) predicted by de Almeida and Thouless[27] for the irreversibility line in the *H-T* diagram of the Ising SG system, suggesting that the line H_{cl} is an irreversibility line of the magnetization. In fact, the derivative $d(\delta\chi)/dT$ shows a local minimum around the line H_{cl}.

Ru-MG undergoes two magnetic phase transitions at T_{cu} ($=16.3 \pm 0.2$ K) and T_{cl} ($=12.8 \pm 0.3$ K). These phase transitions are characterized by the T dependence of χ'', χ_{ZFC}, and χ_{FC}. (i) The absorption χ'' shows a peak at T_{cu} and plateaulike behavior between T_{pl} and T_{pu}, where $T_{pl}<T_{cl}<T_{pu}$. The temperature T_{pl} slightly increases with increasing f, while T_{cu} remains unchanged. (ii) The deviation of χ_{ZFC} from χ_{FC} at low H occurs below a temperature well above T_{cu}. (iii) The susceptibility χ_{ZFC} decreases with decreasing T well below T_{cl}, suggesting the existence of AF order. Similar behaviors are also observed in stage-2 $CoCl_2$ GIC,[15,16] as described in Sec. II A: T_{cu} ($=8.9$ K) and T_{cl} ($=6.8$–7.2 K). The ratio of T_{cu} to T_{cl} ($=1.27$) for Ru-MG is almost the same as that ($=1.31$–1.24) for stage-2 $CoCl_2$ GIC. The origin of phase transitions at T_{cu} and T_{cl} in Ru-MG may be similar to those in stage-2 $CoCl_2$ GIC. Ru layers are formed of Ru clusters. On approaching T_{cu} from the high-T side, Ru magnetic moments come to order ferromagnetically inside clusters. At T_{cu} these FM Ru clusters continue to order over the same layer through intercluster interactions (mainly ferromagnetic), forming 2D FM long-range order. Below T_{cl} a 3D AF phase and a SG phase coexist, forming a RSG phase. The 3D AF phase is formed of the 2D FM layers which are antiferromagnetically stacked along the c axis through a weak AF interplanar interaction. Such a mixed phase is predicted by the mean-field theory of RSG.[20] The origin of the AF interplanar interaction may be due a weak dipole-dipole interaction between magnetic moments of Ru atoms in adjacent layers. In fact, when the direction of the magnetic moments lie in the c plane, the dipole-dipole interaction energetically favors the AF interplanar interaction.

What kind of spin frustration effect occurs in Ru-MG, leading to the RSG-like behavior? There are at least two kinds of competing interactions. One is the intraplanar FM interaction J. The other is the effective AF interplanar interaction, J'_{eff}, which is on the order of $J'(\xi_a/a)^2$, where J' (<0) is the AF interplanar exchange interaction, ξ_a is the in-plane spin-correlation length, and a is the in-plane lattice constant. The growth of the in-plane spin-correlation length ξ_a is partly limited by the existence of Rh clusters. The size of ξ_a may increase in two steps, giving rise to the successive phase transitions at T_{cu} and T_{cl}. Since the in-plane spin-correlation length increases but does not diverge on approaching T_{cl}, the magnitude of the effective AF interaction remains comparable with that of FM intraplanar interaction J. The spin frustration effect occurs as a result of the competition between these two interactions, leading to RSG behavior.

B. FM blocked state in Rh-MG

The T dependence of the relaxation time τ in Rh-MG is shown in the inset of Fig. 12. The least-squares fit of the data to the Arrhenius law given by Eq. (2) yields $\tau_0=(1.08 \pm 0.05)\times 10^{-9}$ sec and $\Delta E_a/k_B=199\pm 7$ K. The value of τ_0 is reasonable for the activation process. The blocking temperature $T_B(\mathrm{dc})$ is estimated as $T_B(\mathrm{dc}) \approx \Delta E_a/25k_B = 8.0$ K, where $\tau_m=10^2$ sec. This value is close to the peak temperature $T_p(\mathrm{ZFC})$. This result indicates that the FM blocked state is formed below $T_p(\mathrm{ZFC})$ in Rh-MG.

In our system the size of Rh clusters is not uniform. Since T_B is different for different sizes, the effect of the distribution function $g(T_B)$ should be considered. The T dependence of $(-dM_{TR}/dT)$ gives a direct measurement to determine the form of $g(T_B)$.[28] The T derivative $(-dM_{TR}/dT)$ shows a broad peak around 5–7 K and reduces to zero around T_f ($=13.5$ K). It is predicted that (i) $T_p(\mathrm{ZFC})$ is lower than T_f for a log-normal distribution function $g(T_B)$

$=[(2\pi)^{1/2}\sigma T_B]^{-1}\exp\{-[\ln(T_B/T_B^0)]^2/2\sigma^2\}$ with a constant T_B^0 and the standard deviation σ and that (ii) T_p(ZFC) is equal to T_f for a rectangular distribution function [$g(T_B)$ = constant for $T_B < T_f$].[23,28] Our result suggests that the log-normal distribution function is appropriate in Rh-MG. In the log-normal distribution function the average of T_B is given by $\langle T_B\rangle = T_B^0\exp(\sigma^2/2)$, the maximum is given by $T_B^{\max} = T_B^0\exp(-\sigma^2)$, and the deviation ΔT_B is given by $\Delta T_B = [\langle T_B^2\rangle - \langle T_B\rangle^2]^{1/2} = \langle T_B\rangle[\exp(\sigma^2)-1]^{1/2}$. In spite of the lack of a model calculation of χ_{FC} vs T based on the distribution, it may be reasonable to assume that T_p(ZFC) (= 9.7 K) is equal to $\langle T_B\rangle$ and T_f (= 13.5 K) is equal to $\langle T_B\rangle + \Delta T_B$. Then the values of σ, T_B^0, and $T_B^{\max}$ are estimated as $\sigma = 0.62$, $T_B^0 = 8.0$ K, and $T_B^{\max} = 5.5$ K. The value of $T_B^{\max}$ is consistent with the peak temperature of the data $(-dM_{TR}/dT)$ vs T.

C. Origin of ferromagnetism in Ru- and Rh-MG's

What is the origin of the 2D ferromagnetism in Ru- and Rh-MG's? Why is the ferromagnetism of Ru-MG much stronger than that of Rh-MG? Krüger *et al.*[12] have discussed the magnetic moment of the Ru monolayer on the graphite C(0001) substrate. The pristine Ru metal has a hexagonal-close-packed (hcp) structure with the lattice constants $a = 2.704$ and $c = 4.292$ Å, while the graphite has a honeycomb structure with the in-plane lattice constant a_G (=2.46 Å). The in-plane lattice constant (a) of Ru atoms is almost twice that of graphite: $2a_G/\sqrt{3} = 2.84$ Å. It is assumed that the Ru layer forms an in-plane structure denoted by the $p(2/\sqrt{3}\times 2/\sqrt{3})R30°$ structure, where the angle between the fundamental lattice vectors of the Ru layer and the graphene layer is 30°. Krüger *et al.*[12] have predicted that the magnetic moment of the Ru atom changes with the interfacial distance d_c between the Ru atoms and the graphene layer. The magnetic moment of the Ru atoms undergoes a steplike increase from $0\mu_B$ to $1.2\mu_B$, when $d_c = 2.39$ Å (=4.5 a.u.) and saturates to $1.9\mu_B$ at $d_c = 2.86$ Å.

In the case of Ru-MG, the Ru monolayer is sandwiched between adjacent graphene layers. Since the c-axis repeat distance I_c is 12.60 Å for the stage-2 $RuCl_3$ GIC, the separation distance between the Ru layer and the graphene layer is 4.625 Å. If the separation distance d_c in Ru-MG is on the same order as that in the $RuCl_3$ GIC, according to Krüger *et al.*,[12] the magnetic moment at $d_c = 4.625$ Å is about $1.9\mu_B$ for the Ru atoms, which satisfies at least the necessary condition for the occurrence of the 2D ferromagnetism in Ru-MG. In contrast, the magnetic moment for Rh/C(0001) is considerably smaller than that for Ru/C(0001), but the overall dependence of the magnetic moments on d_c is quite similar. This prediction is consistent with the superparamagnetic behavior observed in Rh-MG.

VI. CONCLUSION

Ru- and Rh-MG's magnetically behave like quasi-2D ferromagnetic systems because of their unique layered structures. Ru-MG undergoes successive magnetic phase transitions at T_{cu} (=16.3 K) and T_{cl} (=12.8 K). The origin of these phase transitions in Ru-MG is essentially the same as that in stage-2 $CoCl_2$ GIC. The intermediate phase between T_{cu} and T_{cl} is 2D ferromagnetic. The low-temperature phase below T_{cl} may be the mixed phase (RSG phase), where the AF and SG phases coexist. Rh-MG shows a superparamagnetic behavior. A FM blocked state is formed below 9.7 K. The relaxation time obeys the Arrhenius law for thermal activation.

ACKNOWLEDGMENTS

The work at SUNY-Binghamton was supported by SUNY-Research Foundation (Grant No. 240-9522A). The work at Osaka University was supported by the Ministry of Cultural Affairs, Education, and Sport, Japan, under a grant for young scientists (Grant No. 70314375) and by Kansai Invention Center, Kyoto, Japan.

*Email address: suzuki@binghamton.edu
†Email address: Juerg_Walter@t-online.de

[1] V.L. Moruzzi and P.M. Marcus, Phys. Rev. B **39**, 471 (1989).
[2] A.J. Cox, J.G. Louderback, and L.A. Bloomfield, Phys. Rev. Lett. **71**, 923 (1993).
[3] S. Blügel, Phys. Rev. Lett. **68**, 851 (1992).
[4] O. Eriksson, R.C. Albers, and A.M. Boring, Phys. Rev. Lett. **66**, 1350 (1991).
[5] M.J. Zhu, D.M. Bylander, and L. Kleinman, Phys. Rev. B **43**, 4007 (1991).
[6] R. Wu and A.J. Freeman, Phys. Rev. B **45**, 7222 (1992).
[7] S. Blügel, Phys. Rev. B **51**, 2025 (1995).
[8] C. Liu and S.D. Bader, Phys. Rev. B **44**, 12 062 (1991).
[9] G.A. Mulhollan, R.L. Fink, and J.L. Erskine, Phys. Rev. B **44**, 2393 (1991).
[10] R. Pfandzelter, G. Steierl, and C. Rau, Phys. Rev. Lett. **74**, 3467 (1995).
[11] L. Chen, R. Wu, N. Kioussis, and J.R. Blanco, J. Appl. Phys. **81**, 4161 (1997).
[12] P. Krüger, J.C. Parlebas, G. Moraitis, and C. Demangeat, Comput. Mater. Sci. **10**, 265 (1998).
[13] M. Suzuki, CRC Crit. Rev. Solid State Mater. Sci. **16**, 237 (1990).
[14] G. Dresselhaus, J.T. Nicholls, and M.S. Dresselhaus, in *Graphite Intercalation Compounds II*, edited by H. Zabel and S.A. Solin (Springer-Verlag, Berlin, 1992), p. 247.
[15] M. Suzuki and I.S. Suzuki, Phys. Rev. B **58**, 840 (1998).
[16] M. Suzuki and I.S. Suzuki, J. Phys.: Condens. Matter **14**, 5583 (2002).
[17] L. Néel, Ann. Geofis. **5**, 99 (1949).
[18] R.W. Chantrell, M. El-Hilo, and K. O'Grady, IEEE Trans. Magn. **27**, 3570 (1991).
[19] A.T. Ogielski, Phys. Rev. B **32**, 7384 (1985).
[20] H. Takayama, J. Phys. Soc. Jpn. **65**, 1450 (1996).
[21] J. Walter, S. Wakita, W. Boonchuduang, S. Hara, M. Suzuki, and I.S. Suzuki, J. Phys. Chem. B **106**, 8547 (2002).
[22] I.S. Suzuki and M. Suzuki (unpublished).

[23] T. Bitoh, K. Ohba, M. Takamatsu, T. Shirane, and S. Chikazawa, J. Phys. Soc. Jpn. **64**, 1305 (1995).
[24] M. Tokumoto, Y.S. Song, K. Tanaka, T. Sato, and T. Yamabe, Solid State Commun. **97**, 349 (1996).
[25] M. El-Hilo and K. O'Grady, IEEE Trans. Magn. **26**, 1807 (1990).
[26] E.P. Wohlfarth, J. Phys. F: Met. Phys. **10**, L241 (1980).
[27] J.R.L. de Almeida and D.J. Thouless, J. Phys. A **11**, 983 (1978).
[28] E.P. Wohlfarth, Phys. Lett. **70A**, 489 (1979).